Journal of Applied Mathematics and Physics, 2025, 13(10), 3225-3235
https://www.scirp.org/journal/jamp
ISSN Online: 2327-4379
ISSN Print: 2327-4352

# Modelling and Analysis of Rolling Bearing Fault Diagnosis Processes Based on Nonlinear Dynamics

**Zihan Qian**

Jinling High School, Nanjing, China
Email: 13910921634@139.com

**How to cite this paper:** Qian, Z.H. (2025) Modelling and Analysis of Rolling Bearing Fault Diagnosis Processes Based on Nonlinear Dynamics. *Journal of Applied Mathematics and Physics*, **13**, 3225-3235.
https://doi.org/10.4236/jamp.2025.1310184

**Received:** August 26, 2025
**Accepted:** October 11, 2025
**Published:** October 14, 2025



## Abstract

In order to better extract the displacement fault signals inside bearings based on the vibration characteristics of rolling bearings after failure, a two-degree-of-freedom model simplifying the rolling bearing as a lumped mass-elastic system is established. The model fully considers influencing factors such as nonlinear time-varying stiffness and damping caused by bearing defects. Using the Fourier method, dynamic simulations and analyses are conducted for faults in the outer ring, inner ring, and rolling elements of the rolling bearing. The results are largely consistent with theoretical calculations, indicating that the model possesses certain accuracy and practicality in engineering applications.

## Keywords

Rolling Bearings, Defect Size, Vibration Signals, Simulation Analysis

## 1. Introduction

Rolling bearings are common general-purpose components in rotating machinery. According to statistics, 30% of rotating machinery failures are caused by bearing failures. Therefore, successful fault diagnosis and prediction of rolling bearings can reduce unnecessary economic losses and play an important role in ensuring the normal operation of production [1]. Establishing an effective bearing failure simulation engineering model allows for the direct generation of various types of failures as needed, without waiting for natural failures to occur in production. This enables in-depth research into their failure mechanisms and dynamic characteristics, providing more precise diagnostic methods for detecting bearing failures under different operating conditions. Additionally, the signals

generated by the fault simulation model can be used to train neural networks or applied to intelligent diagnostic algorithms such as support vector machines, enabling automatic identification and prediction of bearing fault types. This reduces reliance on the limited availability of fault samples in actual production processes, thereby promoting the development of new methods for bearing fault diagnosis [2].

In bearing fault diagnosis, studying the nonlinear vibration mechanisms of rolling bearings under different defect conditions can provide theoretical guidance for mechanical equipment condition monitoring, process maintenance, and fault diagnosis [3]. Therefore, this paper investigates the relationship between bearing system vibration responses and defect parameters under various defect conditions, analyzes the mathematical relationship between fault characteristic frequencies and raceway defect parameters in the frequency domain, and explores the influence of different defect parameters on rolling bearing system vibration responses through numerical fitting methods.

## 2. Dynamic Modelling of Rolling Bearings

### 2.1. Basic Structure of Bearings

Rolling bearings are precision components widely used in rotating machinery. They convert sliding friction between rotating and stationary components into rolling friction and serve to support loads and guide motion [3]. The basic structure consists of four components: inner ring, outer ring, rolling elements, and cage, as shown in Figure 1. Here, $r_1$ and $r_2$ represent the inner and outer ring raceway radii, respectively; $d$ is the diameter of the rolling elements; $D$ is the bearing pitch diameter; and $\alpha$ is the contact angle.

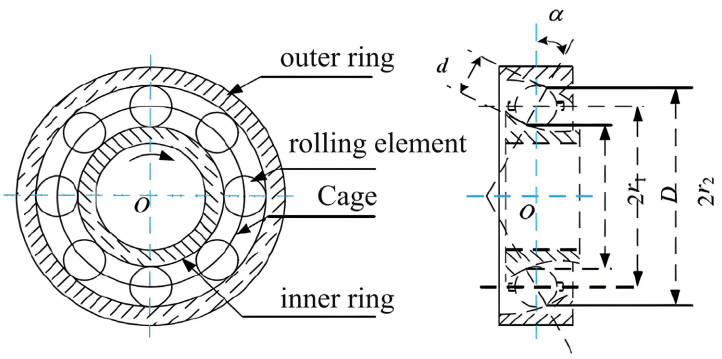


Figure 1. Basic structure of a bearing.

Under normal circumstances, the outer ring of a rolling bearing is fixed to the bearing seat hole, while the inner ring is fixed to the shaft and rotates with it. The rolling elements roll within the cavity formed by the inner and outer rings to maintain relative motion between them. The cage serves to separate the rolling elements, reduce friction and collision, and distribute them uniformly along the circumference, enabling the bearing to bear loads.

## 2.2. Simplification of the Bearing Dynamics Model

This model takes the rolling bearing as the research object. In order to better extract the internal displacement fault signals, the bearing is simplified as a two-degree-of-freedom lumped mass-spring system, as shown in Figure 2. The rotor rotates at a constant speed along the axis, and the rolling bearing is installed on the bearing housing to support the rotation of the rotor [4] [5]. In Figure 2, $K_s$, $K_p$, $C_s$ and $C_p$ represent the combined stiffness and damping of the inner and outer rings of the rolling bearing, respectively. The horizontal and vertical vibration displacements of the inner and outer rings are selected as the generalized coordinates of the system.

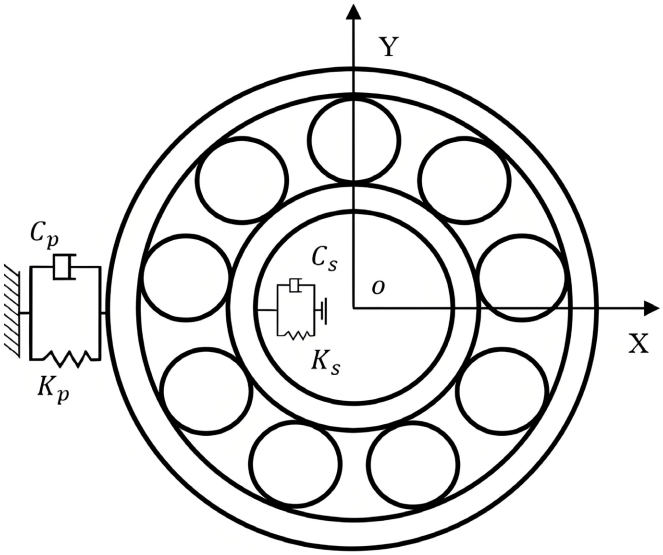


Figure 2. Schematic diagram of the mass-elasticity system model.

The following assumptions are made, taking into account the main contact relationships within the system:

1) The inner ring rotates with the shaft, while the outer ring is fixed to the bearing housing.

2) The inertial forces and gyroscopic torques of the rolling elements are neglected.

3) The bearing is well lubricated, and relative sliding occurs only within the load-bearing zone.

4) The thermal effects caused by friction are neglected.

5) Contact friction is neglected.

6) Only isothermal elastic-fluid lubrication is considered.

In the two-degree-of-freedom dynamic model of rolling bearings, the bearing is simplified as a spring-damping system, and the rolling elements are simplified as nonlinear elastic bodies [6]. Based on Newton's second law, the two-degree-of-freedom nonlinear dynamic equations for angular contact ball bearings can be established as:

$$\begin{cases} m\ddot{\delta}_x + C_b\dot{\delta}_x + K_b\delta_x + F_x = W_x \\ m\ddot{\delta}_y + C_b\dot{\delta}_y + K_b\delta_y + F_y = W_y \end{cases}$$

In the equation, $m$ is the equivalent mass of the rotating component; $C_b$ is the equivalent damping system of the bearing; $K_b$ is the equivalent stiffness of the bearing; $\delta_x$ and $\delta_y$ are the composite displacements of the bearing in the $x$-direction and $y$-direction, respectively; $F_x$ and $F_y$ are the interaction forces in the $x$-direction and $y$-direction within the bearing, respectively; $W_x$ and $W_y$ are the external loads applied to the bearing in the $x$-direction and $y$-direction, respectively.

#### 2.2.1. Simplification of Stiffness and Damping

As shown in Figure 3, the stiffness of the inner and outer rings of a well-lubricated rolling bearing can be considered to consist of two parts: Hertz contact stiffness and oil film stiffness. At the same time, when lubrication is good, a lubricating oil film will form between the rolling elements and the raceway, so the damping part will also consist of two parts: internal damping and oil film damping.

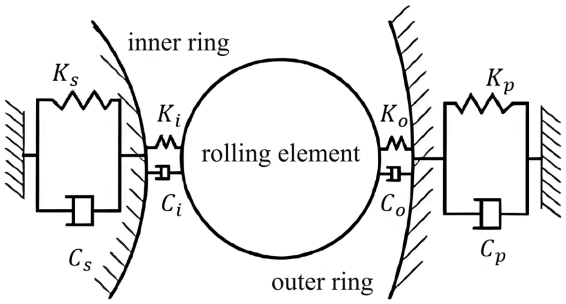


Figure 3. Simplified diagram of inner and outer ring stiffness damping.

Under load, the normal approach between the two raceways separated by the rolling elements and the lubricating oil film is equal to the sum of the approaches between the rolling elements and each raceway. Therefore, the comprehensive stiffness expression obtained by connecting the inner ring stiffness and the outer ring stiffness in series is:

$$K_b = \left[ \frac{1}{\left(1/K_s\right)^{1/n} + \left(1/K_p\right)^{1/n}} \right]^n$$

In the formula, for ball bearings, $n = 3/2$.

Damping is an important parameter in mechanical systems, mainly serving to reduce vibration and amplitude. According to the definition of damping, the damping of the inner and outer rings is expressed by the following formula:

$$\begin{cases} C_s = \left(C_i^{-1} + C_{fi}^{-1}\right)^{-1} \\ C_p = \left(C_o^{-1} + C_{fo}^{-1}\right)^{-1} \end{cases}$$

Further, the comprehensive damping is derived as:

$$C_b = \frac{1}{C_s^{-1} + C_p^{-1}}$$

### 2.2.2. Nonlinear Contact Forces in Bearings

Important parameters of rolling bearings include the number of balls $N_b$, ball diameter *d*, bearing diameter *D*, and contact angle $\alpha$. Typically, the outer ring of a rolling bearing is fixed to the bearing housing, while the inner ring is fixed to the shaft and rotates with the shaft. The balls roll purely in the raceway. The total contact deformation of the *i*-th ball is a function of the relative displacement between the inner and outer rings and the angular position $\varphi_i$ of the *i*-th ball, specifically expressed as:

$$\delta_i = \left(x_n - x_w\right)\cos\varphi_i + \left(y_n - y_w\right)\sin\varphi_i$$

In the formula, $i = 1, 2, \cdots, N_b$; $x_n$、$x_w$ are the horizontal displacements of the inner ring and outer ring of the bearing, respectively, $\delta_x = x_n - x_w$; $y_n$, $y_w$ are the vertical displacements of the inner ring and outer ring of the bearing, respectively, $\delta_y = y_n - y_w$.

Since only the balls in the bearing load zone will experience contact deformation, the following switch function is defined:

$$\gamma_i = \begin{cases} 1 & \delta_i > 0 \\ 0 & \text{otherwise} \end{cases}$$

The angular position of the *i*-th ball is a function of the time interval $dt$, the initial angular position $\varphi_0$ of the cage, and the angular velocity $\omega_c$ of the cage, expressed as:

$$\varphi_i = \frac{2\pi(i-1)}{N_b} + \omega_c dt + \varphi_0$$

$$\omega_c = \left(1 - \frac{d}{D}\right)\frac{\omega}{2}$$

In the formula, $\omega$ is the rotational speed of the axis, $\omega = \frac{2\pi N}{60}$.

In summary, it can be concluded that the total nonlinear contact force of the bearing in the horizontal and vertical directions can be expressed as follows:

$$F_x = k_b \sum \gamma_i \delta_i^{1.5} \cos\varphi_i$$

$$F_y = k_b \sum \gamma_i \delta_i^{1.5} \sin\varphi_i$$

### 2.2.3. Fault Defect Modelling

Bearings that rotate under heavy loads for extended periods of time experience periodic loads at fixed positions, leading to localised fatigue damage. Bearing damage often exhibits a certain width and depth, manifesting as multiple local defects on the raceway surface. The time-varying displacement of rolling bearings during operation may also be altered due to the influence of local defects, as shown in Figure 4. When the defect is located on the inner raceway surface, the defect will sequentially enter and exit the load-bearing zone as the inner ring rotates; when

the defect is located on the outer raceway, its position remains unchanged.

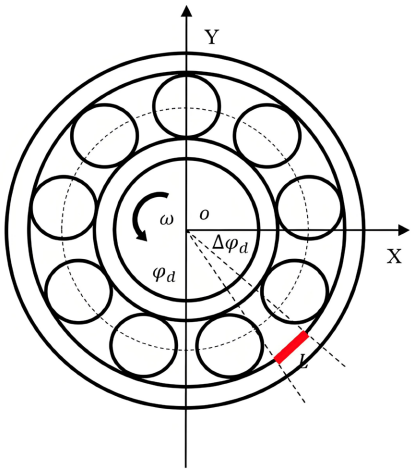


Figure 4. Schematic diagram of bearing outer ring failure.

In Figure 4, the fault width is set to $L$, the depth is $h$, the crossing angle is $\Delta\varphi_d$, and the fault angle position is $\varphi_d$.

When the ball rolls over a local fault, it releases a certain amount of deformation. Define the switch function $\beta_i$ for the occurrence of the fault. At this point, the deformation of the $i$-th rolling element entering the defect can be expressed as:

$$\delta_i = (x_n - x_w)\cos\varphi_i + (y_n - y_w)\sin\varphi_i - c - \beta_i c_d$$

$$\beta_i = \begin{cases} 1 & \varphi_d < \varphi_i < \varphi_d + \Delta\varphi_d \\ 0 & \text{otherwise} \end{cases}$$

Using the above equation, calculate the nonlinear contact force of the bearing. Substitute the nonlinear contact force into the given dynamic differential equation of the bearing to obtain the vibration response of the rolling bearing.

## 3. Vibration Simulation Analysis

Taking a certain type of ball bearing as an example, the main parameters are shown in Table 1.

Table 1. Main parameters of bearings.

| Project | Value | Unit |
|---|---|---|
| Steel ball diameter | 4.76 | mm |
| Pitch circle diameter | 23.5 | mm |
| Radial clearance | −2 | μm |
| Number of steel balls $N_b$ | 9 | individual |
| Contact angle $\alpha$ | 0 | (˚) |
| Outer ring mass | 1.2638 | Kg |
| Damping | 1376 | N·s/m |
| Stiffness | 42410 | N/m |

Among these, the radial load is 500 N, and the spindle speed (inner ring speed) is 1500 r/min, resulting in an inner ring rotational frequency of 25 Hz. For bearings where the inner ring rotates while the outer ring remains stationary, when defects exist on the inner ring raceway or outer ring raceway, the passing frequency of the rolling elements through a defect on the inner ring raceway or outer ring raceway can be determined based on geometric relationships. These are referred to as the inner ring defect frequency and outer ring defect frequency, respectively, and are expressed in Table 2.

Table 2. Defect frequency.

| Fault location | Characteristic frequency |
|---|---|
| Inner ring | $f_i = \frac{N_b}{2}\left(1+\frac{d}{D}\cos\alpha\right)f_r$ |
| Outer ring | $f_o = \frac{N_b}{2}\left(1-\frac{d}{D}\cos\alpha\right)f_r$ |
| Rolling elements | $f_b = \frac{D}{2d}\left[1-\left(\frac{d}{D}\right)^2(\cos\alpha)^2\right]f_r$ |
| Cage | $f_c = \frac{1}{2}\left(1-\frac{d}{D}\cos\alpha\right)f_r$ |

In Table 2, $f_i$, $f_o$, $f_b$ and $f_c$ represent the fault characteristic frequencies of the inner ring, outer ring, rolling elements, and cage, respectively. $d$ is the diameter of the rolling elements, $D$ is the diameter of the pitch circle of the rolling bearing, $\alpha$ is the contact angle, $N_b$ is the number of rolling elements, and $f_r$ is the rotational frequency of the shaft.

Therefore, the defect frequency of the rolling elements is 118.3605 Hz, the defect frequency of the outer ring is 89.7128 Hz, and the defect frequency of the inner ring is 135.2872 Hz.

### 3.1. Analysis of Bearing Failures in Different Areas

To investigate the fault response, local defect characteristics were added to the bearing dynamics model. The simulation under a 500 N radial load produced a vibration response, which was analyzed in the frequency domain using MATLAB's ODE solver and the Fourier method [7].

The resulting signal for a defect size of 0.5 mm wide by 0.25 mm deep is presented in Figure 5.

As shown in Figure 5(a), the time-domain plots of horizontal and vertical accelerations within the 0 - 2 s range clearly exhibit oscillatory curves.

Figure 5(b) shows two acceleration pulse signals generated when the rolling body passes over defects 1 and 2 within the 0.2 - 0.25 s time interval. Based on the rotational direction of the rolling body and the time interval between the acceleration signals, it can be determined that the acceleration pulse signals generated when

the rolling body passes over defect 1 are A1 and A2, and those generated when passing over defect 2 are B1 and B2. Additionally, the time intervals between pulses A1 and A2, and B1 and B2 are approximately 16.89 ms, while the time interval between B1 and A2 is approximately 8.43 ms.

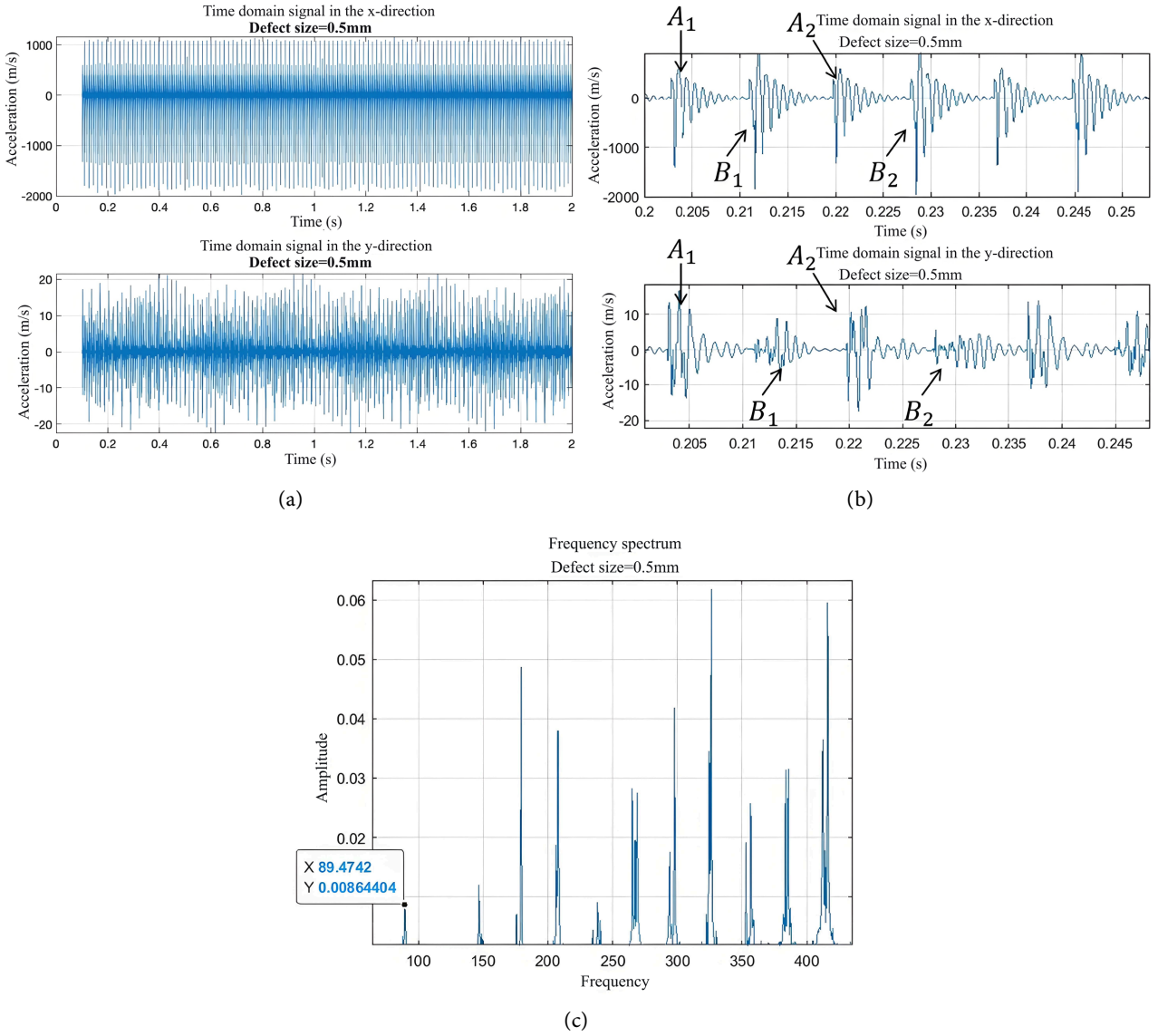


**Figure 5.** (a) 0 - 2 s acceleration time domain diagram; (b) Acceleration time domain diagram at 0.2 - 0.25 s; (c) Outer ring fault spectrum diagram.

As shown in Figure 5(c), by performing envelope analysis on the simulated acceleration signals, the vibration signals in the frequency domain are obtained. Under the initially set fault magnitude, the bearing exhibits a frequency of 89.4727 Hz, which exactly corresponds to the characteristic frequency of an outer ring fault in the bearing. Therefore, based on the demodulated spectrum, it can be determined that the bearing fault is an outer ring fault.

As shown in Figure 5, the amplitude of the acceleration pulse signals generated

when the rolling element rolls over the same defect is almost the same. Additionally, the amplitude of the acceleration pulse signal generated when rolling over defect 2 is greater than that generated when rolling over defect 1. This is because when the rolling element rolls over the two defects sequentially, the acceleration pulse signals A1 and A2 generated when rolling over defect 2 have not yet fully decayed, while the acceleration pulse signals B1 and B2 appear when rolling over defect 1. The undecayed A1 and A2 are superimposed on B1 and B2, respectively, resulting in the amplitudes of pulses B1 and B2 being greater than those of A1 and A2, respectively.

### 3.2. Failure Analysis of Different Defect Parameters

Four different sizes of failures were set using the failure switch function, with outer ring failure sizes of 0.5, 2.0, 3.5, and 5.0 mm, respectively.

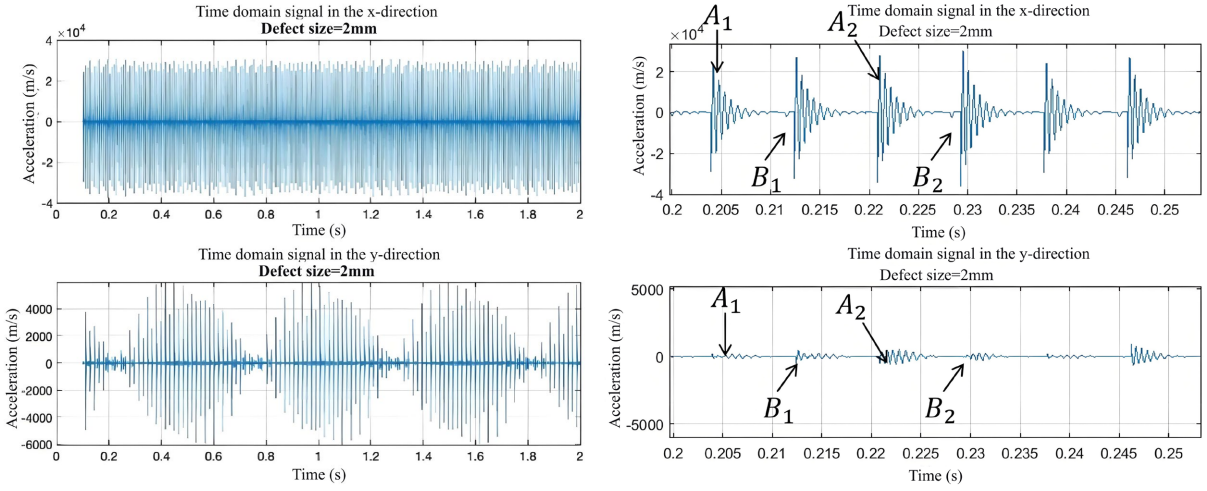


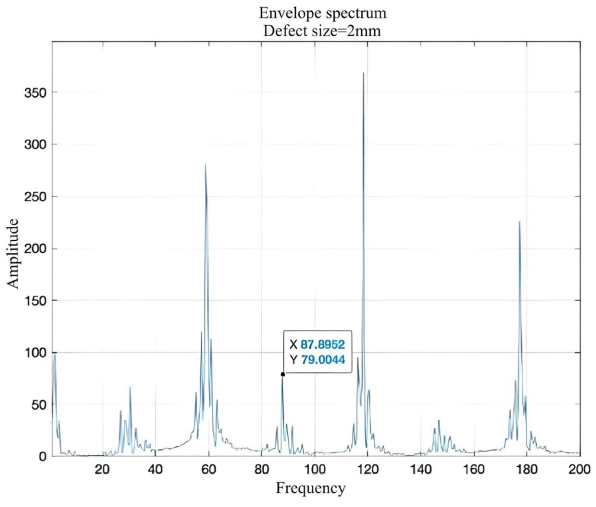


**Figure 6.** (a) Time domain diagram of acceleration from 0 to 2 seconds under a 2 mm defect; (b) Acceleration time domain diagram at 0.2 - 0.25 s under a 2 mm defect; (c) Outer ring failure spectrum under a 2 mm defect.

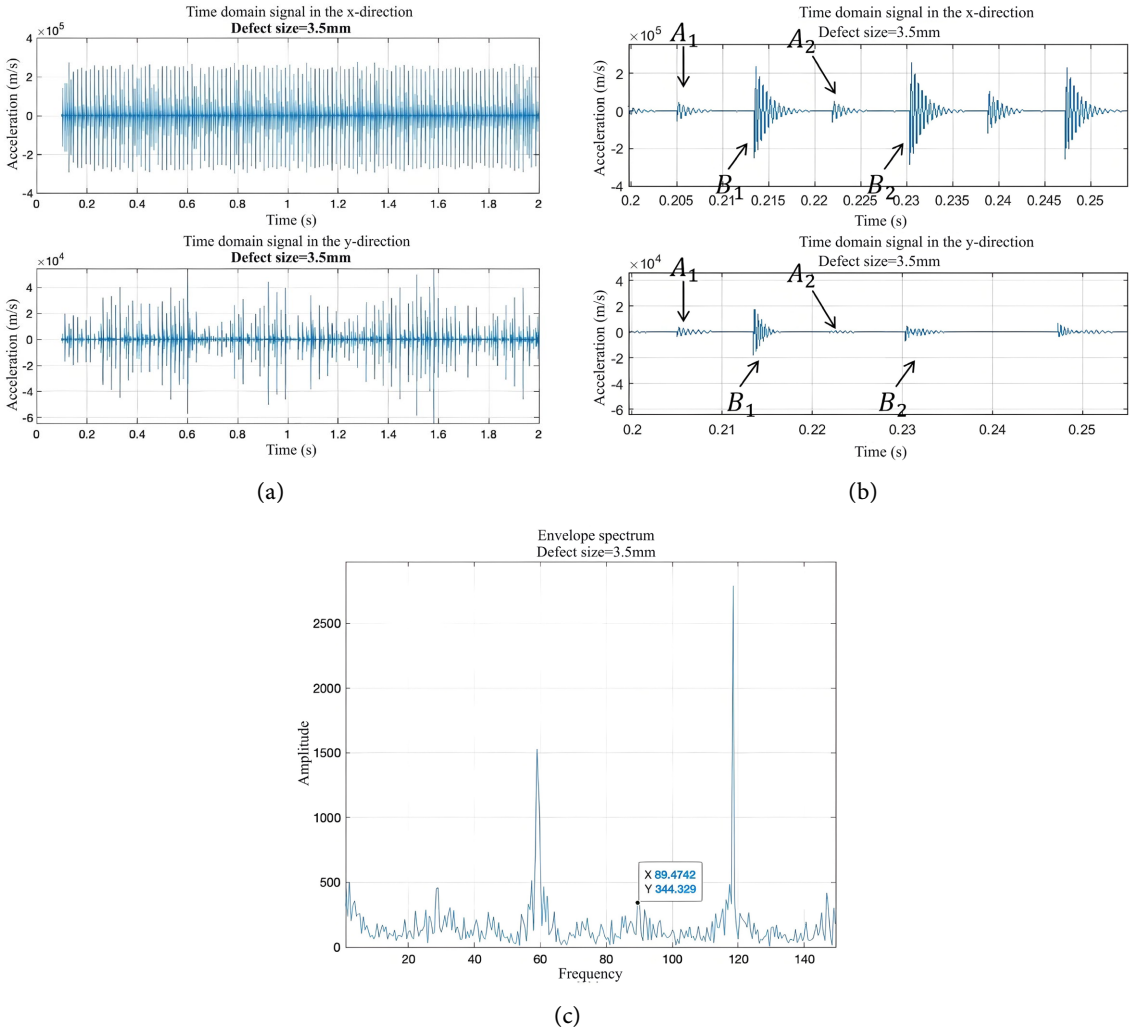


**Figure 7.** (a) Time domain diagram of acceleration from 0 to 2 seconds under a 3.5 mm defect; (b) Acceleration time domain diagram at 0.2 - 0.25 s under a 3.5 mm defect; (c) Outer ring fault spectrum diagram under a 3.5 mm defect.

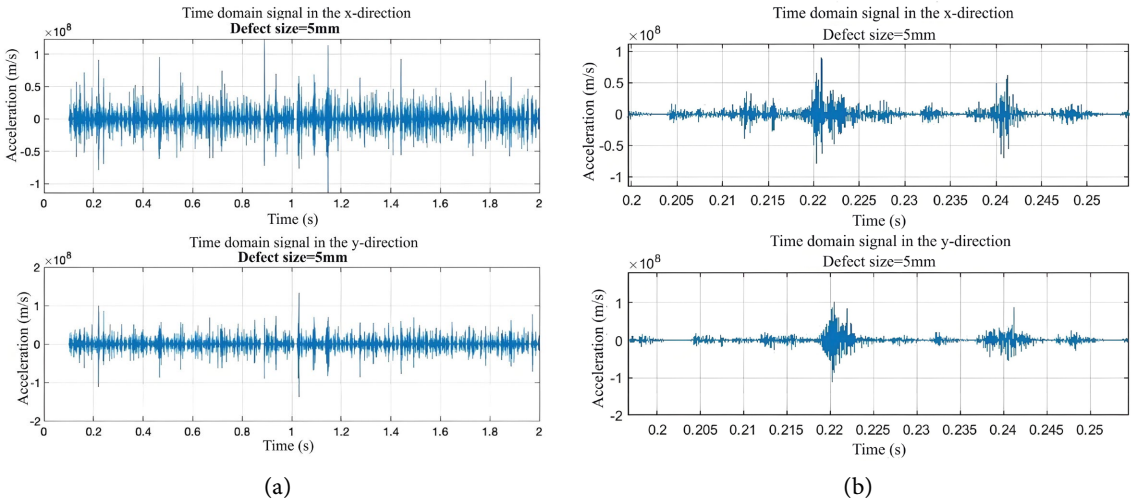


**Figure 8.** (a) Time domain diagram of acceleration from 0 to 2 seconds under a 5 mm defect; (b) Acceleration time domain diagram at 0.2 - 0.25 s under a 5 mm defect.

From Figure 5 to Figure 8, it can be seen that as the defect becomes larger, the impact oscillation becomes more and more obvious, and the fault becomes more and more serious, requiring manual replacement to avoid affecting normal actual use.

## 4. Summary

1) The nonlinear vibration mechanism of rolling bearings under different defects was studied.

2) The relationship between the vibration response of the bearing system and defect parameters under various defect conditions was investigated.

3) The mathematical relationship between the fault characteristic frequency in the frequency domain and the raceway defect parameters was analyzed, and the influence of different defect parameters on the vibration response of the rolling bearing system was explored using numerical fitting methods.

4) The fault model established in this study can provide a theoretical foundation and basis for future monitoring and fault diagnosis of rolling bearings.

## Conflicts of Interest

The author declares no conflicts of interest regarding the publication of this paper.

## References

[1] Wang, G.B., He, Z.J., Chen, X.F., *et al*. (2013) Basic Research on Mechanical Fault Diagnosis: Where to Go from Here. *Journal of Mechanical Engineering*, **49**, 63-72.

[2] Kumbhar, S.G., Sudhagar P, E. and Desavale, R. (2020) An Overview of Dynamic Modeling of Rolling-Element Bearings. *Noise & Vibration Worldwide*, **52**, 3-18. https://doi.org/10.1177/0957456520948279

[3] Liu, J. (2014) Research on Nonlinear Excitation Mechanism and Modelling of Rolling Bearing Defects. Ph.D. Thesis, Chongqing University.

[4] Liu, J., Shao, Y. and Zuo, M.J. (2013) The Effects of the Shape of Localized Defect in Ball Bearings on the Vibration Waveform. *Proceedings of the Institution of Mechanical Engineers, Part K: Journal of Multi-Body Dynamics*, **227**, 261-274. https://doi.org/10.1177/1464419313486102

[5] Li, H.L. (2020) Finite Element Dynamic Modelling and Size Evolution Study of Local Defects in Rolling Bearings. Master's Thesis, Lanzhou University of Technology.

[6] Shan, C.F., Kang, J.X., Yuan, H., *et al*. (2018) Modelling of the Dynamic Response of Rolling Bearing Systems with Local Defects under Elastic Fluid Lubrication and Sliding Conditions. *Vibration and Shock*, **37**, 56-64.

[7] Yan, P., Yan, C., Wang, K., Wang, F. and Wu, L. (2020) 5-DOF Dynamic Modeling of Rolling Bearing with Local Defect Considering Comprehensive Stiffness under Isothermal Elastohydrodynamic Lubrication. *Shock and Vibration*, **2020**, Article ID: 9310278. https://doi.org/10.1155/2020/9310278